

# Oxidative Stress after Subarachnoid Hemorrhage in *gp91<sup>phox</sup>* Knockout Mice

Shimin Liu, Jiping Tang, Robert P Ostrowski, Elena Titova, Cara Monroe,  
Wanqiu Chen, Wendy Lo, Robert Martin, John H Zhang

**ABSTRACT: Background:** Oxidative stress largely contributes to early brain injury after subarachnoid hemorrhage (SAH). One of the major sources of reactive oxygen species is NADPH oxidase, upregulated after SAH. We hypothesized that NADPH oxidase-induced oxidative stress plays a major causative role in early brain injury after SAH. **Methods:** Using *gp91<sup>phox</sup>* knockout (ko) and wild-type (wt) mice, we studied early brain injury in the endovascular perforation model of SAH. Mortality rate, cerebral edema, oxidative stress, and superoxide production were measured at 24 h after SAH. Neurological evaluation was done at 23 h after SAH surgery. **Results:** Genotyping confirmed the existence of a nonfunctional *gp91<sup>phox</sup>* gene in the ko mice. CBF measurements did not show differences in SAH-induced acute ischemia between ko and wt mice. SAH caused a significant increase of water content in the ipsilateral hemisphere as well as an increase of Malondialdehyde (MDA) levels and superoxide production. There were no significant differences in post-SAH mortality rate, brain water content and the intensity of the oxidative stress between knockout and wild type groups of mice. **Conclusions:** Our results suggest that *gp91<sup>phox</sup>* is not critically important to the early brain injury after SAH. An adaptive compensatory mechanism for free radical production in knockout mice is discussed.

**RÉSUMÉ: Le stress oxydatif après une hémorragie sous-arachnoïdienne chez les souris knock-out gp91-phox. Contexte :** Le stress oxydatif contribue de façon importante aux lésions précoces dues à une hémorragie sous-arachnoïdienne (HSA). La NADPH oxydase est une des sources majeures de dérivés réactifs de l'oxygène qui est régulée à la hausse après une HSA. Nous avons émis l'hypothèse que le stress oxydatif induit par la NADPH oxydase est une cause majeure de dommage cérébral après une HSA. **Méthodes :** Nous avons étudié les dommages cérébraux précoces chez le modèle de HSA par perforation endovasculaire chez des souris de phénotype sauvage (ps) et des souris knock-out (ko) gp91-phox. Le taux de mortalité, l'œdème cérébral, le stress oxydatif et la production de superoxyde ont été mesurés 24 heures après l'HSA. L'évaluation neurologique était faite 23 heures après la chirurgie. **Résultats :** Le génotypage a confirmé l'existence d'un gène gp91-phox non fonctionnel chez les souris ko. On n'a pas constaté de différence dans la mesure du débit sanguin cérébral entre les souris ps et les souris ko en phase d'ischémie aiguë induite par l'HSA. L'HSA a causé une augmentation significative du contenu aqueux dans l'hémisphère ipsilatéral ainsi qu'une augmentation des niveaux de malondialdéhyde et de la production de superoxyde. Il n'y avait pas de différences significatives entre les groupes de souris ps et ko quant au taux de mortalité, au contenu aqueux du cerveau et à l'intensité du stress oxydatif post HSA. **Conclusions :** Nos résultats indiquent que gp91-phox ne joue pas un rôle critique dans les dommages cérébraux précoces après une HSA. Nous discutons d'un mécanisme compensatoire d'adaptation pour la production de radicaux libres chez les souris ko.

Can. J. Neurol. Sci. 2007; 34: 356-361

Spontaneous subarachnoid hemorrhage (SAH) represents 5–7% of all strokes,<sup>1,2</sup> and SAH-related mortality reaches 50%.<sup>3–5</sup> Acute cerebral ischemia and subsequent injury are major causes of morbidity after SAH.<sup>3,6</sup> Several studies, including investigations in superoxide dismutase (SOD) transgenic mice, showed that superoxide and other reactive oxygen species (ROS) largely contribute to the early brain injury after SAH.<sup>7–11</sup> NADPH oxidase has been primarily described as responsible for superoxide production in phagocytes.<sup>12</sup> Superoxide is generated on the membrane component *gp91<sup>phox</sup>*,<sup>13–15</sup> which is expressed in all regions of the brain, with prominent localizations in the hippocampus, cortex, amygdale, striatum, and thalamus.<sup>16</sup>

Acutely after SAH, *gp91<sup>phox</sup>* expression is upregulated with an increase of NADPH oxidase-dependent superoxide production in cerebral vessels.<sup>17,18</sup>

From the Department of Physiology and Pharmacology (SL, JT, RPO, ET, CM, WC, WL, JHZ), Department of Neurosurgery (JHZ), Department of Anesthesiology (RM, JHZ), Loma Linda University, Loma Linda, CA, USA.

RECEIVED NOVEMBER 22, 2006. ACCEPTED IN FINAL FORM APRIL 16, 2007.

Reprint requests to: J.H. Zhang, Department of Physiology & Pharmacology Riskey Hall, Room 219, Loma Linda University School of Medicine, Loma Linda, California, 92350, USA

Ischemic injury has been found to be reduced in mice lacking a functional NADPH oxidase.<sup>19</sup> It is also believed that global ischemia due to an increase in intracranial pressure after SAH contributes to early brain injury after SAH.<sup>8</sup> Moreover, a previous report from our lab showed that decreased NADPH oxidase expression by hyperbaric oxygen therapy reduced neuronal injury and improved functional performance.<sup>20</sup>

Our hypothesis is that NADPH oxidase plays a major role in mediating early brain injury after subarachnoid hemorrhage. In this study, using an endovascular perforation model of SAH, we studied early brain injury in *gp91<sup>phox</sup>* knockout (ko) and wild-type (wt) mice.

## MATERIALS AND METHODS

All experimental procedures complied with the Guide for the Care and Use of Laboratory Animals (NIH) and have been approved by the Animal Care and Use Committee at Loma Linda University.

### Transgenic mice

Wild-type (C57BL/6) and *gp91<sup>phox</sup>* knockout (*gp91<sup>phox</sup>* ko) mice that lack the membrane gp91<sup>phox</sup> catalytic subunit of NADPH oxidase were bred in the animal facility at Loma Linda University Medical Center. The breeders were obtained from Jackson Laboratories (Bar Harbor, ME, USA). All *gp91<sup>phox</sup>* ko and age-matched wild-type mice were males and were studied at 12–20 weeks of age. Before surgery, animals were encoded as Group A and Group B. The surgeon and observant did not know the code until after statistic analysis (double-blind method). This code was revealed through PCR genotyping as the last step of this project.

### Genotyping

Genotyping was done as previously described.<sup>21</sup> The following primers were used to genotype *gp91<sup>phox</sup>* ko mice: primer for wild-type allele, 5'-AAGAGAACTCCTC TGCTGTGAA-3'; primer for disrupted allele, 5'-GTTCTAATTCCATCAGAAGCTTATCG-3'; common primer, 5'-CGCACTGGAACCCCTGAGAAAGG-3'. The 240-bp wild-type product and 195-bp product from the disrupted *gp91* allele were amplified using the following conditions: 94°C for 30 s, 56°C for 30 s, 72°C for 30 s. The cycle was repeated 35 times. PCR products were separated on 1.5% agarose gel and stained with ethidium bromide.

### Animal model

The SAH model was induced according to Parra's description<sup>22</sup> with some modifications. Briefly, animals were anesthetized using ketamine/xylazine (100/10 mg/kg b.w.; i.p.). A blunted 5-0 monofilament nylon suture was introduced into the external carotid artery and advanced through the internal carotid artery to the right anterior cerebral artery (ACA) near the anterior communicating artery, where resistance was encountered. The filament was advanced 5 mm further to perforate ACA, then immediately withdrawn. In the sham surgery the filaments were advanced without arterial perforation. In subsets of both wt and ko mice (n=6 each) CBF was measured by means of laser Doppler flowmeter (PeriFlux System 5000,

Perimed, Jarfalla, Sweden) in the acute period after perforation of the artery. Body temperature was kept constant (37.5 ± 0.5 °C) during the operation and for two hours afterwards.

### Neurological evaluation

Neurological evaluation was performed at 23 h after perforation using a 27-point scale<sup>22</sup> and a newly-composed 36-point scale as described in the Table.

### Brain water content

Brains were harvested and quickly separated into left and right hemispheres and cerebellum at 24 h after SAH.<sup>23</sup> Brain samples were weighed before and after drying in an oven at 105°C for 24 h. After 24 h, samples were weighed again and water content was calculated according to the following formula: Water content = [wet weight - dry weight]/wet weight\*100%

### Malondialdehyde (MDA) and superoxide production

Under deep anesthesia, mouse brains were perfused with PBS at 24 h after SAH. The level of MDA in the whole brain tissue was measured using an LPO-586 kit (Oxis Research) as previously described.<sup>24</sup>

*In vivo* superoxide production was measured using the dihydroethidium (DHE) method. Dihydroethidium stock solution was prepared at a concentration of 100 mg/ml in dimethylsulfoxide (DMSO), which was further diluted to a working condition of 1 mg/ml in PBS containing 20% DMSO before using. At 23 h post-SAH, a jugular vein injection of DHE was done at a dosage of 3 mg/kg. Ninety min later, injection animals were perfused with PBS and perfusion-fixed with 10% formalin. Brains were post-fixed in 10% formalin for 24 h. Coronal sections of 50 microns were made using a vibratome. DHE reacts with superoxide and fluoresces at Ex 510–550 nm and Em 580 nm. After reaction with superoxide, DHE emitted an ethidium-like (Et-like) fluorescence. Seven fields from the areas with greatest fluorescence from each animal were photographed under 20x objective lens of the OLYMPUS BX51 microscope using 1822 ms exposure time. The positive signal for superoxide was separated from the background of digital microphotographs using the histogram function with a pixel threshold setting of 150–255 on red color. The area of superoxide signal was measured and expressed as square micrometer per 20x field (Image-Pro Plus 4.5.1.22).

### Statistical analysis

All quantitative data were expressed as means ± SEM. One way ANOVA was used to verify a statistical significance of differences between means, followed by Scheffe's test for multiple comparisons. For analysis of performance data, Kruskal-Wallis ANOVA and Dunn's test were used. A P value < 0.05 was considered significant.

## RESULTS

### Genotyping

The band for NADPH oxidase *gp91<sup>phox</sup>* subunit is located at 240 bp in wild-type mice but shifted to 195 bp in ko mice (Figure 1A). 195bp polymerase chain reaction (PCR) product from *gp91-*

**Table: 36-point scale for neurological evaluation after SAH**

Tests	Scores			
	0	1	2	3
<b>1. Alertness</b>	No response	Response to pain	Response to touch	Response to sound
<b>Motor function</b>				
2. Spontaneous activity (5 min)	No walking	Walks without wall approaching	Approaches 1-2 walls	Approaches 3-4 walls
3. Symmetry of walking	Falls while walking	Circling to one side	Turns to one side while pulling tail	Walking straight
4. Head/neck movement when suspended on tail	Turns <45 degree to both sides	Turns <45 degree to one side	Turns >45 degree to both sides	Turns >90 degree
5. Symmetry of forelimbs when suspended on tail	One front limb flexion	One front paw flexion	One front limb partial outreach	Symmetrical outreach
6. Climbing	Slides down within 2 seconds	Holds without climbing	Climbing with difficulty	Steady climbing
7. Balance on rod	Falls within 2 seconds	Holds without walking	Walking with difficulty	Steady walking
<b>Sensory function</b>				
8. Q-tip to Vibrissae	No head turning on both sides	No head turning on one side	Decreased response (one or both side)	Instant bilateral head turn
9. Q-tip to neck	No head turning on both sides	No head turning on one side	Decreased response (one or both side)	Instant bilateral head turn
10. Pin stick to body sides	No response on both side	One side no response	Decreased response (one or both side)	Instant bilateral response
11. Pinch to ears	No response on both side	One side no response	Decreased response (one or both side)	Instant bilateral response
<b>Reflex</b>				
12. Corneal reflex	No blinks on both sides	No blink on one side	Decreased response	Instant bilateral blinks

ko mice represents a disrupted gene which is not functioning as a neomycin resistance gene was inserted into exon 3. In the study of Pollock and colleagues the Western blot analysis on extracts of neutrophil-rich peritoneal exudate cells from hemizygous male mice confirmed that no detectable protein was expressed.<sup>25</sup> Genotyping revealed that group A was the *gp91<sup>phox</sup>* knockout group and group B was the wild-type group.

### Animal model

Ninety-six animals were used to induce the SAH model, and 30 animals served as sham control in this study. The 95.8% (92/96) animals had successful SAH which was confirmed by observing blood clots in the subarachnoid space at post mortem. Post mortem examination of mice brains revealed blood clots in the vicinity of the anterior communicating artery. Massive hemorrhages, however, covered the entire circle of Willis as specified in our grading system. SAH severity was graded as minimal, mild, middle, and severe with the clot being a single spot, less than 25% of base, 25% to 75% of base, and more than

75% of base, respectively. In the *gp91<sup>phox</sup>* knockout group, 41% (19/46) and 37% (17/46) had mild and middle-sized clots in subarachnoid space. In the wild-type group 39% (18/46) and 43% (20/46) had mild and middle-sized clots in subarachnoid space. The number of minimal clots (less than 25% of base as described above) was 5 and 3 in the wt and ko group, respectively. The number of severe clots was 1 and 7 in wt and ko mice, respectively. The analysis of CBF after SAH revealed no differences in CBF decrease between ko and wt animals (data not shown). At 24 h post-SAH surgery, 14.6% (14/96) animals died of SAH. Nine mice died in the *gp91<sup>phox</sup>* knockout group and 5 in the wild-type group ( $p > 0.05$ ). Most deaths occurred between 6-24 h after SAH surgery, from severe cerebral edema and middle-sized clots.

### Neurological evaluation

As shown in Figure 1 panel B, the neurological score in the SAH group was significantly lower than that of the sham group.

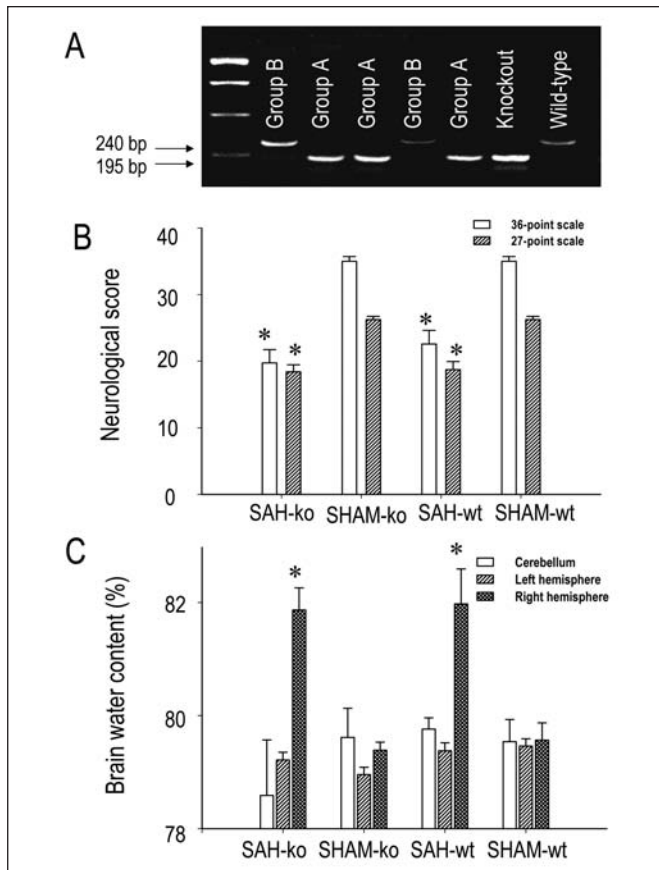


**Figure 1:** Genotyping, neurological score, and brain water content. **A.** Genotyping. NADPH oxidase *gp91<sup>phox</sup>* subunit shown as a 240 bp band in wt mice (Group B) but shifted to 195 bp in ko mice (Group A). **B.** Neurological score at 23 h post-surgery in SAH and SHAM groups of ko and wt mice; expressed as median scores. Neurological scores in SAH groups were significantly lower than that of SHAM groups, however they did not differ between ko and wt mice. **C.** Brain water content in SAH and SHAM groups did not show a difference between ko and wt mice. Asterisks,  $p < 0.05$  compared with corresponding SHAM group. NS, not significant (SAH-ko vs. SAH-wt).  $N = 20$  in each SAH group, but  $N = 5$  in each SHAM group.

There was no significant difference in neurological scores between *gp91<sup>phox</sup>* knockout and wild-type groups on both scales.

#### Brain water content

As shown in Figure 1 panel C, at 24 h after SAH, brain water content increased in the ipsilateral hemisphere and was significantly higher than in the contralateral, left hemisphere. There was also no significant difference in water content between the *gp91<sup>phox</sup>* knockout and wild-type groups of mice after SAH.

#### MDA and superoxide production

The basal level of MDA production was approximately 7 pmoles/mg protein in ko and wt SHAM groups (Figure 2A).

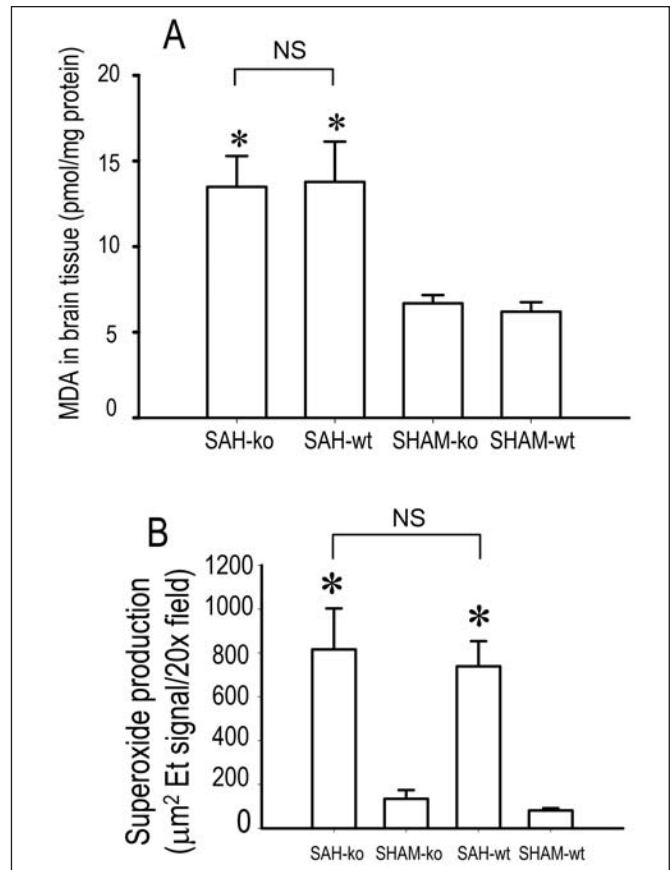


**Figure 2:** Malondialdehyde (MDA) levels and superoxide production in cerebral cortex. **A.** MDA levels significantly increased at 24 h after SAH in ko and wt mice with no difference found between these two groups. Asterisks,  $p < 0.05$  compared with corresponding SHAM group.  $N = 12$  in each SAH group, but  $N = 6$  in each SHAM group. **B.** SAH animals showed similarly high Et-like signals in ko and wt groups at 24 h post-surgery. The Et-signal-positive areas in SAH groups were significantly larger than that of SHAM groups indicating a prominent superoxide production (B). Asterisks,  $p < 0.05$  compared with corresponding SHAM group. NS, not significant (SAH-ko vs. SAH-wt).  $N = 8$  in each SAH group, but  $N = 4$  in each SHAM group.

MDA levels doubled the basal levels in both groups at 24 h after SAH. There was no difference in MDA levels between ko and wt animals within SHAM and SAH groups at 24 h after surgery.

Superoxide production, as measured by the area of positive Et-like signal/20x field, increased significantly at 24 h after SAH. There was no difference in superoxide production between *gp91<sup>phox</sup>* knockout and wild-type groups (Figure 2B).

#### DISCUSSION

The similar degree of SAH severity in both groups suggested a consistent model. SAH resulted in deteriorated neurological function, increased cerebral edema, and oxidative stress. However, in this study *gp91<sup>phox</sup>* knockout did not cause a reduction in oxidative stress and brain edema, suggesting that

*gp91<sup>phox</sup>* is not critically important to the early brain injury after SAH. Genotyping results confirmed *gp91<sup>phox</sup>* gene disruption and the band pattern was identical with the one previously reported.<sup>21</sup> Although the other measures of oxidative stress might have been more sensitive in this model, the lack of differences in lipid breakdown markers, superoxide production, brain water content and functional performance is consistent with a similar extent of oxidative stress in wt and ko groups after SAH. In addition no significant difference in baseline oxidative stress levels was found between Sham groups with wild-type or *gp91<sup>phox</sup>* knockout mice in this study, which is consistent with reports in other systems.<sup>26,27</sup>

Interestingly, in our recent study with an intracerebral hemorrhage model, *gp91<sup>phox</sup>* knockout mice showed less bleeding as well as reduced damage and oxidative stress as compared to wild-type mice.<sup>21</sup> However, unlike in ICH, in the SAH model *gp91<sup>phox</sup>* ko has no effect on hemorrhage size. Additionally, the potential compensatory mechanisms in the SAH model are likely activated by global ischemia and sustained hypoperfusion, which are not typical for ICH.

It has been reported that *gp91<sup>phox</sup>* gene knockout can induce adaptive changes during an animal's growth.<sup>28</sup> When one gene has been deleted, other related genes may alter in order to compensate for this gene deletion.<sup>29</sup> An alternative *gp91<sup>phox</sup>* isoform, Nox4, has been found upregulated after aortic constriction<sup>28</sup> in *gp91<sup>phox</sup>* knockout mice and in focal cerebral ischemia<sup>30</sup> of wild-type mice. Moreover, Frantz et al<sup>31</sup> found that oxidative stress and myocardial NOX 1 expression were increased in *gp91<sup>phox</sup>* knockout mice of the coronary artery ligation model. Expression of Nox 4 and Nox 1 in the brain have been previously reported.<sup>16,30,32</sup> It is possible that a compensatory upregulation of Nox 4 and/or Nox 1 occurred during breeding in our study. NADPH oxidase may also interact with other factors responsible for ROS production. Therefore, lipoxygenases, cytochrome p450, xanthine oxidase and eNOS might be upregulated in *gp91<sup>phox</sup>* gene knockout mice. Alternatively, intrinsic antioxidants such as SOD may also have altered during the adaptive changes of knockout mice's growth.

This study shows no benefits of knocking out the *gp91<sup>phox</sup>* gene for protection against early brain injury after SAH. It also suggests a limited value of knocking out a single gene for studying complex mechanisms of oxidative stress acutely after SAH. However, since infiltrating inflammatory cells produce excess ROS via NADPH oxidase containing 91<sup>phox</sup>,<sup>12</sup> it is possible that in the later phase after SAH, 91<sup>phox</sup> knockout would be beneficial by reducing the extent of injury in sites of brain inflammation.

#### ACKNOWLEDGMENTS

This study is partially supported by grants from Department of Anesthesiology at Loma Linda University, from NIH NS52492 to J. Tang and NS53407, NS45694, NS43338, and HD43120 to J. Zhang, and by NIH NCMHD 5P20MD001632.

#### REFERENCES

- Broderick JP, Brott T, Tomsick T, Huster G, Miller R. The risk of subarachnoid and intracerebral hemorrhages in blacks as compared with whites. *N Engl J Med*. 1992;326:733-6.
- Kassell NF, Sasaki T, Colohan AR, Nazar G. Cerebral vasospasm following aneurysmal subarachnoid hemorrhage. *Stroke*. 1985;16:562-72.
- Broderick JP, Brott TG, Duldner JE, Tomsick T, Leach A. Initial and recurrent bleeding are the major causes of death following subarachnoid hemorrhage. *Stroke*. 1994;25:1342-7.
- Kaptain GJ, Lanzino G, Kassell NF. Subarachnoid haemorrhage: epidemiology, risk factors, and treatment options. *Drugs Aging*. 2000;17:183-99.
- Weir B, Macdonald RL, Stoodley M. Etiology of cerebral vasospasm. *Acta Neurochir Suppl*. 1999;72:27-46.
- Bederson JB, Germano IM, Guarino L. Cortical blood flow and cerebral perfusion pressure in a new noncraniotomy model of subarachnoid hemorrhage in the rat. *Stroke*. 1995;26:1086-91.
- Cahill WJ, Calvert JH, Zhang JH. Mechanisms of early brain injury after subarachnoid hemorrhage. *J Cereb Blood Flow Metab*. 2006;26:1341-53.
- Ostrowski RP, Colohan AR, Zhang JH. Molecular mechanisms of early brain injury after subarachnoid hemorrhage. *Neurol Res*. 2006;28:399-414.
- Sehba FA, Bederson JB. Mechanisms of acute brain injury after subarachnoid hemorrhage. *Neurol Res*. 2006;28:381-98.
- Kamii H, Kato I, Kinouchi H, Chan PH, Epstein CJ, Akabane A, et al. Amelioration of vasospasm after subarachnoid hemorrhage in transgenic mice overexpressing CuZn-superoxide dismutase. *Stroke*. 1999;30:867-71.
- Matz PG, Copin JC, Chan PH. Cell death after exposure to subarachnoid hemolysate correlates inversely with expression of CuZn-superoxide dismutase. *Stroke*. 2000;31:2450-9.
- El-Benna J, Dang PM, Gougerot-Pocidallo MA, Elbim C. Phagocyte NADPH oxidase: a multicomponent enzyme essential for host defenses. *Arch Immunol Ther Exp (Warsz)*. 2005;53:199-206.
- DeLeo FR, Quinn MT. Assembly of the phagocyte NADPH oxidase: molecular interaction of oxidase proteins. *J Leukoc Biol*. 1996;60:677-91.
- Segal AW, Abo A. The biochemical basis of the NADPH oxidase of phagocytes. *Trends Biochem Sci*. 1993;18:43-7.
- Decoursey TE, Ligeti E. Regulation and termination of NADPH oxidase activity. *Cell Mol Life Sci*. 2005;62:2173-93.
- Serrano F, Kolluri NS, Wientjes FB, Card JP, Klann E. NADPH oxidase immunoreactivity in the mouse brain. *Brain Res*. 2003;988:193-8.
- Kim DE, Suh YS, Lee MS, Kim KY, Lee JH, Lee HS, et al. Vascular NAD(P)H oxidase triggers delayed cerebral vasospasm after subarachnoid hemorrhage in rats. *Stroke*. 2002;33:2687-91.
- Shin HK, Lee JH, Kim KY, Kim CD, Lee WS, Rhim BY, et al. Impairment of autoregulatory vasodilation by NAD(P)H oxidase-dependent superoxide generation during acute stage of subarachnoid hemorrhage in rat pial artery. *J Cereb Blood Flow Metab*. 2002;22:869-77.
- Walder CE, Green SP, Darbonne WC, Mathias J, Rae J, Dinauer MC, et al. Ischemic stroke injury is reduced in mice lacking a functional NADPH oxidase. *Stroke*. 1997;28:2252-8.
- Ostrowski RP, Tang J, Zhang JH. Hyperbaric oxygen suppresses NADPH oxidase in a rat subarachnoid hemorrhage model. *Stroke*. 2006;37:1314-8.
- Tang J, Liu J, Zhou C, Ostanin D, Grisham MB, Neil Granger D, et al. Role of NADPH oxidase in the brain injury of intracerebral hemorrhage. *J Neurochem*. 2005;94:1342-50.
- Parra A, McGirt MJ, Sheng H, Laskowitz DT, Pearlstein RD, Warner DS. Mouse model of subarachnoid hemorrhage associated cerebral vasospasm: methodological analysis. *Neurol Res*. 2002;24:510-6.
- Ostrowski RP, Colohan AR, Zhang JH. Mechanisms of hyperbaric oxygen-induced neuroprotection in a rat model of subarachnoid hemorrhage. *J Cereb Blood Flow Metab*. 2005;25:554-71.
- Kusaka I, Kusaka G, Zhou C, Ishikawa M, Nanda A, Granger DN, et al. Role of AT1 receptors and NAD(P)H oxidase in diabetes-aggravated ischemic brain injury. *Am J Physiol Heart Circ Physiol*. 2004;286:H2442-51.

25. Pollock JD, Williams DA, Gifford MA, Li LL, Du X, Fisherman J, et al. Mouse model of X-linked chronic granulomatous disease, an inherited defect in phagocyte superoxide production. *Nat Genet.* 1995;9:202-9.
26. Chamseddine AH, Miller FJ Jr. Gp91phox contributes to NADPH oxidase activity in aortic fibroblasts but not smooth muscle cells. *Am J Physiol Heart Circ Physiol.* 2003;285:H2284-9.
27. Gao HM, Liu B, Hong JS. Critical role for microglial NADPH oxidase in rotenone-induced degeneration of dopaminergic neurons. *J Neurosci.* 2003;23:6181-7.
28. Byrne JA, Grieve DJ, Bendall JK, Li JM, Gove C, Lambeth JD, et al. Contrasting roles of NADPH oxidase isoforms in pressure-overload versus angiotensin II-induced cardiac hypertrophy. *Circ Res.* 2003;93:802-5.
29. Thyagarajan T, Totey S, Danton MJ, Kulkarni AB. Genetically altered mouse models: the good, the bad, and the ugly. *Crit Rev Oral Biol Med.* 2003;14:154-74.
30. Vallet P, Charnay Y, Steger K, Ogier-Denis E, Kovari E, Herrmann F, et al. Neuronal expression of the NADPH oxidase NOX4, and its regulation in mouse experimental brain ischemia. *Neuroscience.* 2005;132:233-8.
31. Frantz S, Brandes RP, Hu K, Rammelt K, Wolf J, Scheuermann H, et al. Left ventricular remodeling after myocardial infarction in mice with targeted deletion of the NADPH oxidase subunit gp91PHOX. *Basic Res Cardiol.* 2006;101:127-32.
32. Takeya R, Taura M, Yamasaki T, Naito S, Sumimoto H. Expression and function of Nox1gamma, an alternative splicing form of the NADPH oxidase organizer 1. *FEBS J.* 2006;273:3663-77.